A. O. Brightman[1]
B. P. Rajwa[2]
J. E. Sturgis[3]
M. E. McCallister[1]
J. P. Robinson[1,3]
S. L. Voytik-Harbin[1,3]
[1] *Department of Biomedical Engineering, Purdue University, West Lafayette, IN, USA*

[2] *Department of Biophysics, Institute of Molecular Biology, Jagiellonian University, Krakow, Poland*

[3] *Department of Basic Medical Sciences, School of Veterinary Medicine, Purdue University, West Lafayette, IN, USA*

Received 24 August 1999; accepted 3 April 2000

Time-Lapse Confocal Reflection Microscopy of Collagen Fibrillogenesis and Extracellular Matrix Assembly In Vitro

Abstract: *The development of the next generation of biomaterials for restoration of tissues and organs (i.e., tissue engineering) requires a better understanding of the extracellular matrix (ECM) and its interaction with cells. Extracellular matrix is a macromolecular assembly of natural biopolymers including collagens, glycosaminoglycans (GAGs), proteoglycans (PGs), and glycoproteins. Interestingly, several ECM components have the ability to form three-dimensional (3D), supramolecular matrices (scaffolds) in vitro by a process of self-directed polymerization, "self-assembly". It has been shown previously that 3D matrices with distinct architectural and biological properties can be formed from either purified type I collagen or a complex mixture of interstitial ECM components derived from intestinal submucosa. Unfortunately, many of the imaging and analysis techniques available to study these matrices either are unable to provide insight into 3D preparations or demand efforts that are often prohibitory to observations of living, dynamic systems. This is the first report on the use of reflection imaging at rapid time intervals combined with laser-scanning confocal microscopy for analysis of structural properties and kinetics of collagen and ECM assembly in 3D. We compared time-lapse confocal reflection microscopy (TL-CRM) with a well-established spectrophotometric method for determining the self-assembly properties of both purified type I collagen and soluble interstitial ECM. While both TL-CRM and spectrophotometric techniques provided insight into the kinetics of the polymerization process, only TL-CRM allowed*

Correspondence to: S. L. Voytik-Harbin; email: voytik@ecn.purdue.edu

Biopolymers, Vol. 54, 222–234 (2000)

qualitative and quantitative evaluation of the structural parameters (e.g., fibril diameter) and 3D organization (e.g., fibril density) of component fibrils over time. Matrices formed from the complex mixture of soluble interstitial ECM components showed an increased rate of assembly, decreased opacity, decreased fibril diameter, and increased fibril density compared to that of purified type I collagen. These results suggested that the PG/GAG components of soluble interstitial ECM were affecting the polymerization of the component collagens. Therefore, the effects of purified and complex mixtures of PG/GAG components on the assembly properties of type I collagen and interstitial ECM were evaluated. The data confirmed that the presence of PG/GAG components altered the kinetics and the 3D fibril morphology of assembled matrices. In summary, TL-CRM was demonstrated to be a new and useful technique for analysis of the 3D assembly properties of collagen and other natural biopolymers which requires no specimen fixation and/or staining. © 2000 John Wiley & Sons, Inc. Biopoly 54: 222–234, 2000

Keywords: *extracellular matrix; collagen gel; self-assembly; confocal microscopy; time lapse; reflection; imaging; three-dimensional; fibrillogenesis; submucosa*

INTRODUCTION

Synthetic and biologically derived polymers play a crucial role in the design and engineering of new therapeutic and diagnostic devices for medical applications such as tissue restoration and replacement (i.e., tissue engineering). Synthetic polymers have been obvious candidates for such applications because their chemical and physical properties can be controlled. However, these materials often lack the ability to signal (orchestrate) fundamental cellular processes including adhesion, migration, differentiation, and proliferation. With hopes of increased biocompatibility and elicitation of a desirable cellular response, biomaterials have been fashioned also from tissues and biologically derived molecules (e.g., collagen and glycosaminoglycans). In fact, many of the molecules that compose the extracellular matrix (ECM) of tissues exhibit the ability to polymerize and form complex, three-dimensional (3D) supramolecular assemblies in vitro, a process known as "self-assembly". Although cells are known to play an important role in guiding this assembly process in vivo, it is apparent that much of the information that determines the proper structure of these matrices is contained within the macromolecules that form these structures. We are interested in these self-assembly properties and the fundamental interactions between macromolecules of the ECM, including collagens, proteoglycans (PGs), and glycosaminoglycans (GAGs). Such information will be vital to the synthesis from natural biopolymers of new biomaterials (e.g., gels and matrices) with defined architecture, mechanical properties, and biological signaling capacity.

To date, information on the self-assembly mechanisms of ECM molecules has been obtained using spectrophotometry,[1,2] electron microscopy (EM),[3–5] and dark-field microscopy[6,7] techniques. For example, spectrophotometric measurements of collagen fibril formation (fibrillogenesis) by turbidity provide time course or kinetic details, but yield no direct information about the structural nature of the assembling components. Structural aspects of assembled matrices under steady-state or fixed conditions can be observed using EM; however, extensive specimen preparation and processing are necessary due to vacuum operation of the instrumentation and often result in structural artifacts.[8–10] Although dark-field microscopy has been used to view growth of individual collagen fibrils over time in vitro, this technique is limited in its capacity to image 3D architecture. Indeed, such techniques have been instrumental in elucidating the structural organization and binding interactions of individual collagen, PG, and GAG components of the ECM. However, these techniques have been limited to noncomplex systems and provide only two-dimensional (2D) structural or kinetic information. With time-lapse confocal reflection microscopy (TL-CRM), changes in fibril and matrix structure can be monitored in 3D over time, allowing more direct studies of collagen fibrillogenesis and the molecules that affect this process.

Reflection, or the back-scattering of light, is an intrinsic optical property of many biopolymers, including collagen. When combined with confocal microscopy, reflection images taken at sequential focal planes along the z axis can be reconstructed three-dimensionally for visualization and/or analytical purposes. No chemical processing, physical sectioning, or staining of the specimen is required. The generation of high-resolution images using this technique requires only that a specimen possess either high reflectance (albedo) or substantial changes in index of refraction at its boundaries.[11] For example, this technique was applied by Semler and co-workers to visualize and quantitate the microtopography of porous

biomaterials prepared from synthetic polymers.[12] Likewise, we and others have applied confocal reflection microscopy for surface and volume visualization of 3D matrices prepared from natural biopolymers such as collagen.[8,13] Reflected light from an assembled collagen matrix also has been collected simultaneously with fluorescence from cells stained with vital fluorochromes in a time-lapse mode to monitor the dynamic process of cell migration through a 3D collagen matrix.[8] Herein, we provide the first account of CRM in a time-lapse mode for studying, in three or four dimensions, collagen fibril formation and ECM assembly in vitro. With TL-CRM, both kinetic and 3D structural information can be collected simultaneously as ECM components polymerize from a soluble phase to form an insoluble fibrous matrix or gel.

An elucidation of the component molecules of ECM and how they interact in 3D to form connective tissue scaffolds with tissue-specific structure and function is just in its infancy. Many of our studies have focused on an intact interstitial ECM derived from porcine small intestine which consists of a dense network of cross-linked collagen bundles richly endowed with GAG and PG molecules.[9,14,15] Component molecules of this intact ECM can be solubilized and used to reconstitute a 3D interstitial ECM in vitro. In vitro studies show that the reconstituted interstitial ECM has distinct structural and biological properties compared to reconstituted matrices formed from purified type I collagen alone.[9] These observations led to the hypothesis that PG/GAG components present in the interstitial ECM are contributing to the unique structural and functional properties demonstrated by the reconstituted matrix. In this study we applied TL-CRM to determine and compare the 3D architecture and assembly properties of reconstituted matrices prepared with either purified type I collagen or interstitial ECM components. The usefulness of TL-CRM was further explored by investigating the effect of purified and complex mixtures of PG and GAG components on the assembly process of these matrices. Parallel studies were conducted using the traditional spectrophotometric-based turbidity assay and the insights provided by this technique and TL-CRM are compared and discussed.

MATERIALS AND METHODS

Preparation of 3D Reconstituted Matrices

Purified type I collagen from bovine dermis (Vitrogen) was obtained as a sterile solution in 0.012 N HCl from Collagen Corporation, Fremont, CA. Purified preparations of the GAG, heparin, and the PG, decorin, were obtained from Elkins-Simm, Inc., and Sigma Chemical Co., respectively. Reconstituted interstitial ECM was prepared from porcine small intestinal submucosa (SIS) as described previously.[9] In brief, SIS was powdered under liquid nitrogen and the powder stirred into 0.5*M* acetic acid (5% w/v) containing 0.1% (w/v) pepsin for 72 h at 4°C. The suspension was centrifuged at 12,000 xg for 20 min at 4°C to remove undissolved tissue particulate and dialyzed extensively against 0.01*M* acetic acid. To prepare a solution of solubilized interstitial ECM devoid of PG and GAG components, the powdered intestinal submucosa was first extracted with 4*M* guanidine in 0.5*M* Tris, pH 7.2 for 24 h at 4°C to remove endogenous PGs and GAGs. The tissue pellet was recovered by centrifugation, reextracted, rinsed with acetic acid, and solubilized as above. Water-soluble PGs and GAGs were recovered from the extract supernatant by dialysis and lyophilized. To polymerize (reconstitute) the soluble collagen or interstitial ECM components into a 3D matrix, each solution was diluted and brought to physiologic pH and ionic concentration by the addition of 10× phosphate-buffered saline (PBS) and appropriate concentrated HCl and NaOH solutions. Neutralized solutions were kept at 4°C prior to the initiation of polymerization, which was induced by raising the temperature to 30–37°C. Complete matrix assembly occurred within 10–60 min depending upon the solution composition and polymerization conditions.

Confocal Reflection Microscopy

Unstained 3D matrices of type I collagen or mixtures of interstitial ECM components were polymerized in a Lab-Tek chambered coverglass (Nalge Nunc Int.) and imaged using a BioRad MRC1024 confocal microscope via a 60×, 1.4 NA oil immersion lens. Optical settings were established and optimized on reconstituted matrices after polymerization was complete. An aliquot of a soluble collagen or interstitial ECM preparation was then placed onto the heated (37°C) stage of the microscope, and fibrillogenesis and fibril assembly imaged. Samples were illuminated with 488 nm laser light and the reflected light detected with a photomultiplier tube (PMT) using a blue reflection filter. For the BioRad MRC1024 confocal microscope, instrument setup involved a beamsplitter placed in position D1 and a dichroic filter that reflects 488 nm light into PMT2 in position D2 (Figure 1). Optical filters may be added in positions W1 and W3 for the simultaneous collection of fluorescence information in PMT1 and PMT3, respectively. A z step of 0.2 μm was used to optically section the samples. Because the resolution of the z plane is less than that of the x–y plane, the sampling along the z axis may be different from that of the x–y. 2D (e.g., x–y) or 3D (e.g., x–y–z) sections demonstrating fibrillogenesis and assembly events were recorded at step intervals ranging from 1 to 5 s for up to 1 h. Minimum time intervals required for image collection were dependent on the section size, resolution, and scanning mode. For standardization of scanning depth,

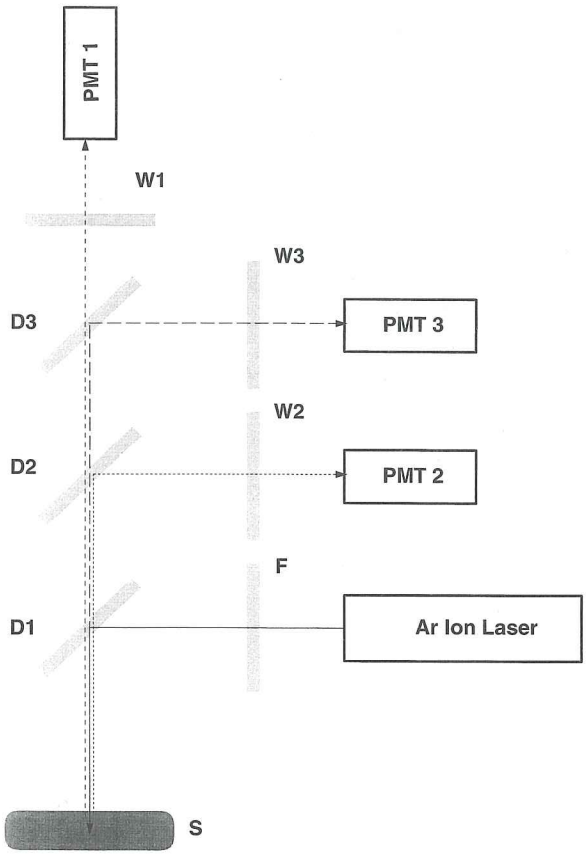

FIGURE 1 Confocal microscope demonstrating filter (D, W, and F) and photomultiplier tube (PMT) positions.

the scanhead was adjusted to a distance in the range of 20–50 μm from the upper surface of the coverglass.

Nonuniform background caused by interference and reflection from the optical pathway was removed from the images using standard rank leveling procedures on each x–y section. Rank leveling consisted of applying a multiple number of erosions followed by a gaussian filter to each section to create a background approximation. This background approximation was then subtracted from the original section to enhance the signal-to-noise ratio. Three-dimensional images of the matrices were either compiled into a single view projection using Laser Sharp (BioRad, Hemel Hempstead, UK) image-processing software or compiled into a 3D projection using Voxel-View reconstruction software (Vital Images). Rank leveling can also be performed on 3D images prior to reconstruction into 3D views to improve image quality. To perform rank leveling in 2D, we used public domain Unix image-processing toolsets: "imgstar" by Steve Winder and "pbmplus" by Jef Poskanzer. A "tcsh" script was used to automate the image-processing tasks. Time-lapse image files were assembled into SGI movie format (sgimv) or MPEG movie format using dmconvert, a standard converter for digital media, a part of Irix 6.2 operating system on a Silicon Graphics Indigo2 workstation. Because MPEG movie formatting involves lossy compression, this format was used for presentation purposes only.

Spectrophotometric (Turbidity) Analysis

Polymerization or fibrillogenesis was monitored in a Lambda 3B UV-VIS spectrophotometer (Perkin-Elmer) equipped with a temperature-controlled, 6-position holder. Absorbance measurements at 405 nm were recorded at 30 s intervals for up to 120 min.

Determination of Total Protein

The total protein content of type I collagen and interstitial ECM solutions was determined using bicinchoninic acid (BCA) reagent (Pierce). Appropriate dilutions of collagen and interstitial ECM were prepared in 0.01M acetic acid or PBS and assayed in triplicate according to methods described previously.[16] Reactions were heated to 60°C for 30 min and absorbance at 562 nm determined. Bovine serum albumin (40–1000 μg/mL) was used to prepare a standard curve.

Determination of Total Collagen

The collagen content of type I collagen and interstitial ECM solutions was estimated using the Sirius Red assay.[17] Appropriate dilutions of collagen and interstitial ECM were prepared and assayed in triplicate. Samples were added to Direct Red 80 dye (50 μM) in 0.5M acetic acid, shaken for 30 min, and centrifuged at 12,000× g for 15 min. Sample pellets were washed in 0.5M acetic acid and resuspended in 0.1 N NaOH. The absorbance at 540 nm was then determined. Purified type I collagen was used to prepare a standard curve in the range of 40–1000 μg/mL.

Determination of Total Glycosaminoglycan/Proteoglycan Content

The PG/GAG content of type I collagen and interstitial ECM solutions was determined using the alcian blue assay as previously described.[18] Samples were assayed in triplicate. Porcine-derived heparin (Elkin-Simms, Inc.) was used to prepare a standard curve in the range of 1–20 heparin units/mL.

Quantitative Analysis of TL-CRM

At present, high-throughput computer algorithms are being developed to facilitate the quantitation of fibril assembly kinetics as well as structural properties, including fibril diameter, fibril density, fibril curvature, and fibril orientation. As a first approach to obtain kinetic information from TL-CRM data, average pixel values were calculated for each 2D image of a time-lapse series and plotted against time.

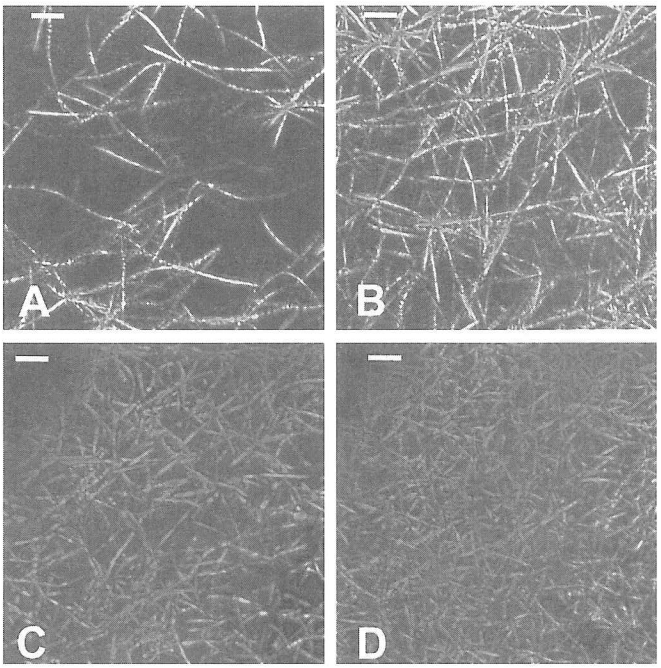

FIGURE 2 Confocal reflection images demonstrate the architectural differences between matrices prepared from type I collagen (A, B) and a complex mixture of interstitial ECM components (C, D). Self-assembly of the matrices was conducted at collagen concentrations of 0.5 mg/mL (A, C) and 1.5 mg/mL (B, D). Bar = 5 μm.

For fibril diameter determinations, a total of 40 fibrils were randomly selected (10 fibers per quadrant) from a z series of images representing an assembled matrix. Using Voxel-View reconstruction software, a threshold was determined for the z series and the images binarized. Five lines were then drawn perpendicular to the long axis of each fibril using the trace feature of the software. The average number of white pixels traversed by the five lines (representing the fiber diameter) was determined and converted into nanometers based upon pixel dimensions. An analysis of variance was conducted on the fibril diameter values obtained for the matrices using the SAS Statistical Software package (SAS Institute Inc., Cary, NC). The Student Newman Keuls method for multiple comparisons ($p < 0.05$) was then applied.

RESULTS

Three-dimensional reconstituted matrices were formed either from purified type I collagen or from partially purified interstitial ECM components of small intestinal submucosa and compared using time-lapse confocal reflection imaging and a spectrophotometric-based turbidity assay. Taken together, these techniques demonstrated disparity between the two matrices with regard to their 3D structural and assembly properties. The architectural differences observed with TL-CRM (Figure 2) were as dramatic as seen previously using scanning electron microscopy (SEM), confirming the dependence of matrix structure on composition.[9] More specifically, when observed using TL-CRM, the fibrils of type I collagen exhibited a larger diameter and greater degree of curvature compared to those of interstitial ECM matrix. Quantitative analysis of the assembled matrices showed that fiber diameters within type I collagen matrices (508 $\pm$ 117 nm) were significantly greater ($p < 0.05$) than those within interstitial ECM (459 $\pm$ 117 nm; Figure 3).

An increase in fibril density with increasing collagen concentration was suggested by the increase in spectrophotometric-based optical density (OD) measurements observed for both matrices (Figure 4). In both cases, the dependence of fibril density on collagen concentration was compared and confirmed visually in 3D by TL-CRM. However, despite the lower net change in turbidity measurements at 405 nm, the fibrils of the interstitial ECM appeared more densely packed compared to those of the purified collagen matrix when analyzed by TL-CRM.

The lag phase of fibrillogenesis was much shorter and the polymerization rate was increased for the interstitial ECM when compared with that of purified

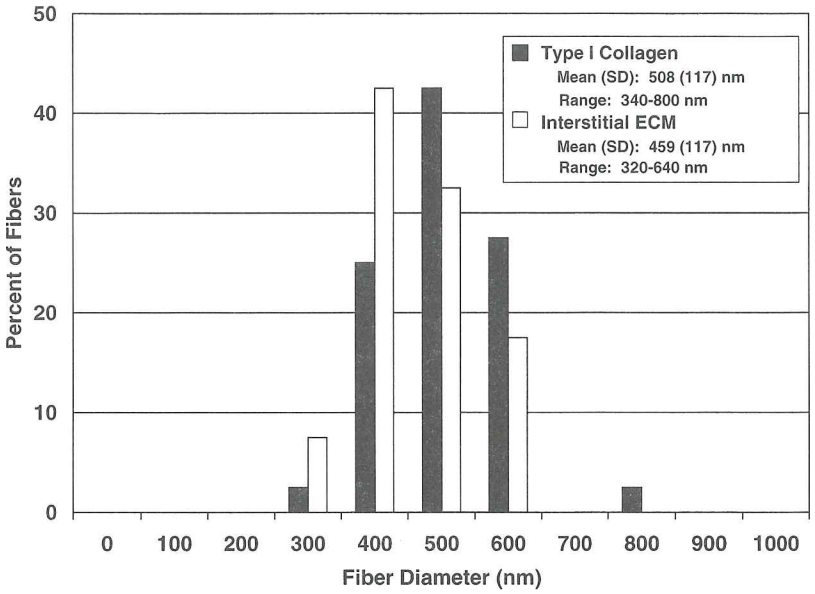

FIGURE 3 Fibril diameter distribution for matrices prepared from type I collagen and a complex mixture of ECM components. The mean diameter of component fibrils of type I collagen matrices was significantly greater than that observed for interstitial ECM ($p < 0.05$).

type I collagen. This was evident in results obtained from both the turbidity assay and the time-lapse imaging (Video 1 and Video 2; website: http://www.cyto.purdue.edu/biopolymer/videos.htm).

Computer-aided 3D reconstruction of CRM images allowed visualization of component fibrils as well as their spatial distribution (Figure 5). The range of fibril diameters quantitated from CRM was 300–800 nm for the type I collagen matrices. This range of fibril diameters is similar to those reported by Friedl using CRM to image assembled collagen matrices.[8] For matrices prepared using air-drying and standard critical point drying techniques and visualized using SEM, average fibril diameters were significantly di-

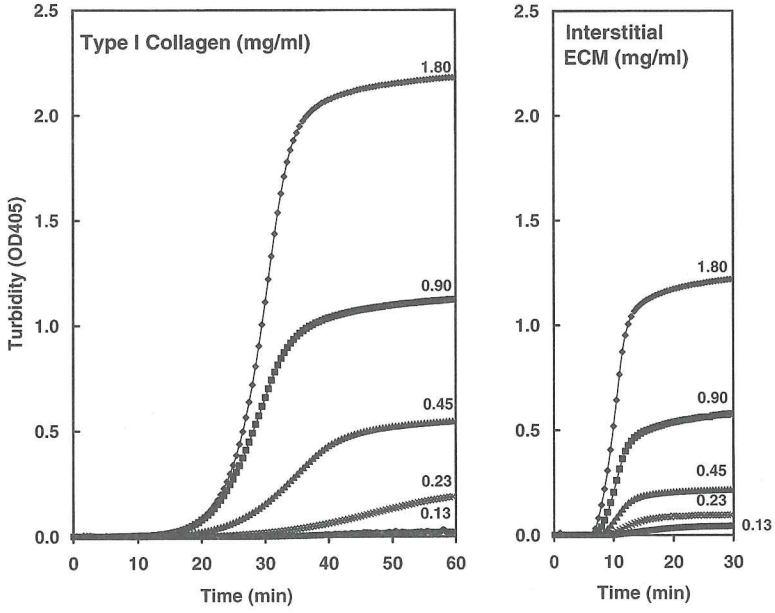

FIGURE 4 Spectrophotometric turbidity measurements of fibrillogenesis and matrix assembly of type I collagen and interstitial ECM at collagen concentrations ranging from 0.13 to 1.8 mg/mL.

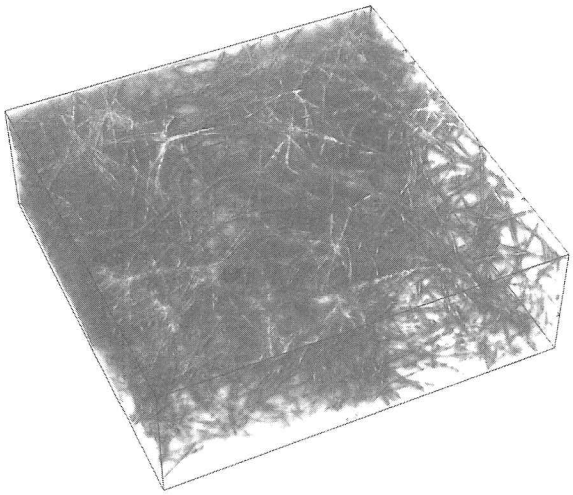

FIGURE 5 Representative 3D reconstructed image of an assembled matrix prepared from a complex mixture of interstitial ECM components.

minished and architectural discrepancies noted.[8,9] Only when analyzed by cryo-stage SEM, in which the specimen is viewed in a quick-frozen hydrated state, were the fibril diameters similar to those observed with TL-CRM.[9]

To evaluate the effects of GAG and/or PG molecules on the assembly differences observed between type I collagen and interstitial ECM, both TL-CRM and the turbidity assay were used to determine the effect of adding heparin, a common GAG of ECM, and decorin, a small proteoglycan of ECM, on matrix assembly and architecture of type I collagen. Collagen fibrils formed in the presence of increasing concentrations of heparin showed a progressive increase in diameter and decrease in density as detected by TL-CRM (Figure 6). Based upon quantitative analysis of CRM, no difference was observed in type I collagen fibril diameters upon addition of low levels of heparin (0.5 U/mL). Alternatively, type I collagen fibrils formed in the presence of higher levels of heparin, 6 U/mL, showed a significant ($p < 0.05$) increase in diameter from 508 ± 117 to 594 ± 124 nm (Figure 7).

Kinetic analyses obtained from spectrophotometric data showed that the addition of heparin to type I collagen resulted in a decrease in lag time, increase in polymerization rate, and increase in optical density (plateau phase; Figure 8). These effects of heparin on collagen assembly were closely matched with the data from the TL-CRM kinetic analysis (Figure 9). Interestingly, the increase in optical density measurements and average pixel values observed with increasing heparin concentration did not correlate with fibril density as determined with TL-CRM.

A decrease in vibrational motion during polymerization as well as a decrease in fibril curvature after polymerization was complete were evident from the analyses by TL-CRM and suggested that collagen matrices formed in the presence of heparin consisted of more rigid fibrils (Video 3, website: http://www.cyto.purdue.edu/biopolymer/videos.htm). These observations were not detectable with the spectrophotometric-based assay. Also evident in TL-CRM, but not the turbidity assay, were the increased number of nucleation sites for fibril initiation and increased fibril bundling induced by heparin.

Analysis of the effect of a proteoglycan on assembly properties was achieved by addition of a small proteoglycan, decorin, to the purified collagen solution. A comparison of two ratios of collagen to decorin in the turbidity assay demonstrated that only at the lower ratio (20:1, higher decorin concentration) was the previously reported effect of decreased rate of collagen fibril assembly observed (Figure 10). This is consistent with the proposed role of decorin in regulating the ordered assembly of fibrils.[19–22] Analysis of the effects of decorin by TL-CRM demonstrated that

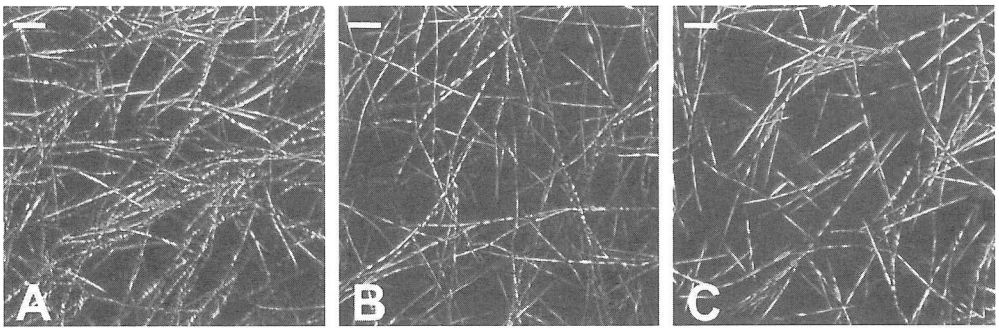

FIGURE 6 Confocal reflection images of type I collagen matrices at a collagen concentration of 1.0 mg/ml formed in the presence of heparin at 0 U/mL (A), 0.5 U/mL (B), and 6 U/mL (C). Bar = 5 μm.

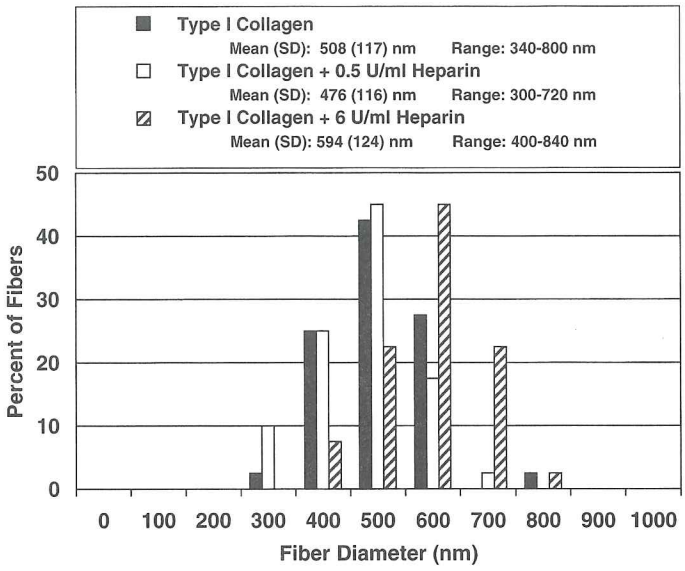

FIGURE 7 Fibril diameter distribution for type I collagen matrices prepared in the presence of heparin at 0, 0.5, and 6 U/mL. Type I collagen fibers formed in the presence of 6 U/mL heparin showed a significant increase in fiber diameter ($p < 0.05$).

in contrast to the effects of heparin, the addition of the small proteoglycan decorin at either concentration, did not significantly alter the size or shape of the fibrils in the completely assembled matrix (Figure 11).

To further understand the effects of PG and GAG components on interstitial ECM assembly and architecture, endogenous PG and GAG were removed from the starting tissue (intestinal submucosa) by extraction with 4*M* guanidine prior to preparation of the solubilized interstitial ECM (ECM−). Three-dimensional reconstruction of TL-CRM images revealed that reconstituted interstitial ECM prepared from tissue in which the PG/GAG components were still present (ECM+) contained fibrils that were increased in density, but decreased in diameter and length, compared to those of matrices in which the PG/GAG compo-

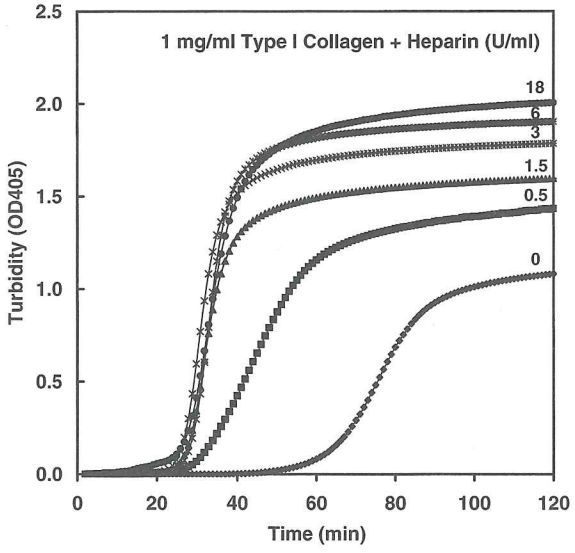

FIGURE 8 Spectrophotometric turbidity measurements of fibrillogenesis and matrix assembly of type I collagen at a collagen concentration of 1.0 mg/mL in the presence of heparin at concentrations ranging from 0 to 18 U/mL.

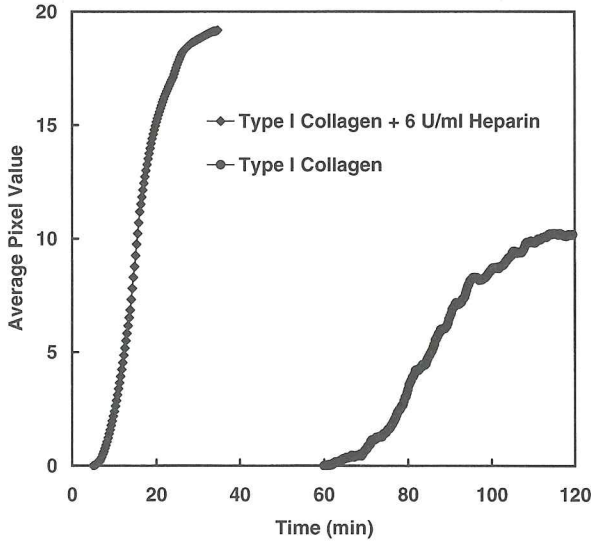

FIGURE 9 Average pixel value of TL-CRM images plotted against time to demonstrate the polymerization kinetics of type I collagen alone and in the presence of 6 U/mL heparin.

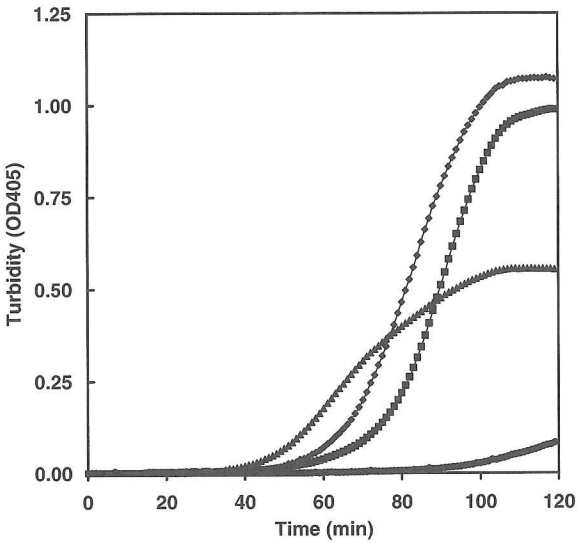

FIGURE 10 Spectrophotometric turbidity measurements of fibrillogenesis and matrix assembly of 1.0 mg/mL collagen alone, ◆; 1.0 mg/mL collagen and 12.5 μg/mL decorin, ■; 0.5 mg/mL collagen alone, ▲; and 0.5 mg/mL collagen and 25 μg/decorin, ●.

nents were removed from the starting material (Figure 12). In fact, interstitial ECM polymerized in absence of the PG/GAG components appeared similar to matrices prepared with type I collagen alone. The increased change in OD exhibited by ECM− in the turbidity assay again was not predictive of the fibril density observed by TL-CRM.

Comparison of the kinetic parameters for ECM− and ECM+ by TL-CRM and the turbidity assay showed only subtle differences in the initiation and rates of fibrillogenesis (Figure 13A). Upon addition of increasing concentrations of extracted PG/GAG components to the ECM− solution, a progressive increase in the lag time (nucleation) and a decrease in rate of fibrillogenesis were observed (Figure 13B). However, in these experiments, the addition of extracted PG/GAG components back to ECM− did not result in a complete restoration of turbidity or structural properties observed with ECM+. These findings suggest that other ECM components that regulate fibrillogenesis and assembly may have been lost during the extraction and dialysis process.

DISCUSSION

The assembly, disassembly, and reassembly of collagen-based extracellular matrices are dynamic processes that occur in vivo during morphogenesis, growth, and repair.[23] The capacity of ECM molecules to self-assemble in vitro has been the root of basic science investigations regarding ECM (tissue) structure and function and is now receiving increased interest for tissue engineering and medical device applications. Collagen is a major constituent of ECM in vivo and perhaps the most important molecule in stabilization of tissue structure. Collagen fibrils aggregate to form fibers or fiber bundles which in turn are organized into tissue-specific architecture such as ropes (tendons and ligaments) or interwoven meshes (dermis). Several factors contribute to the regulation of collagen fibril organization[23] both in vivo and in vitro, including (1) primary structural determinants in the collagen molecule, (2) molar ratios and spatial distributions of molecular types of collagen within a

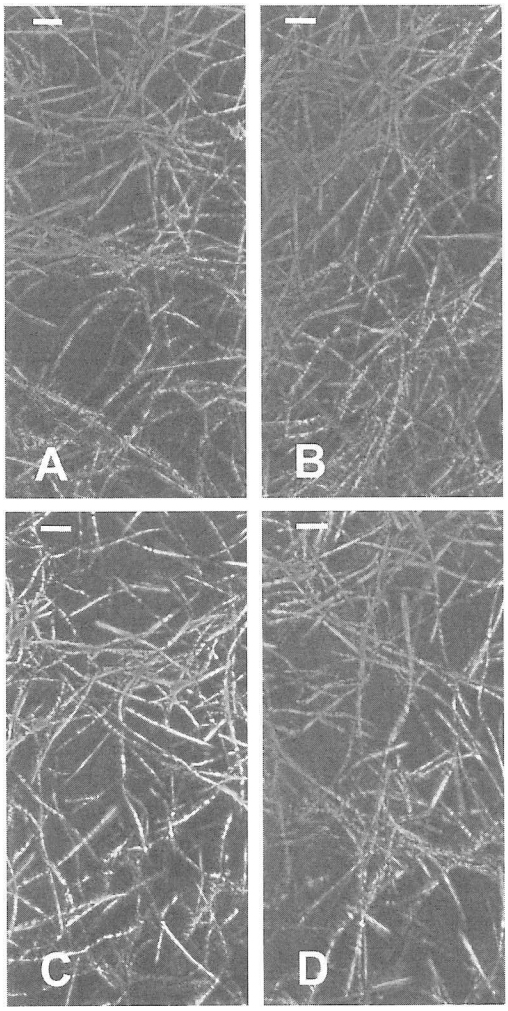

FIGURE 11 Confocal reflection images of type I collagen matrices formed in the presence of decorin. Collagen solutions at 1.0 mg/mL (A) or 0.5 mg/mL (C) were polymerized alone or in the presence of decorin at 12.5 μg/mL (B) or 25 μg/mL (D), representing decorin:collagen rations of 1:80 and 1:20, respectively.

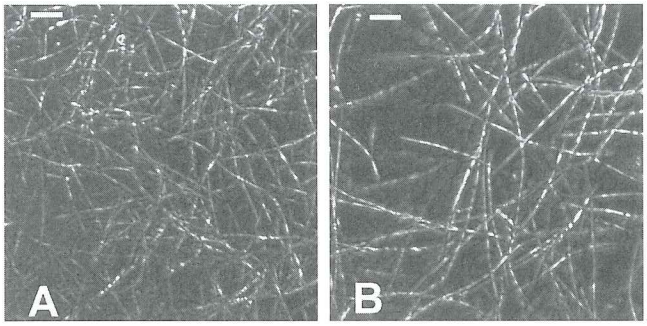

FIGURE 12 Confocal reflection images of interstitial ECM at collagen concentration of 0.5 mg/ml in the presence (A) or absence (B) of PG/GAG components. Bar = 5 μm.

fibril, (3) molar ratios and spatial distributions of noncollagenous macromolecules associated with the fibril, (4) rates and extent of processing of N-terminal and C-terminal non-triple-helix sequences; and (5) assembly conditions. Unfortunately, assembly algorithms that partition and position these molecules in 3D space resulting in the formation of functional connective tissues or scaffolds have yet to be defined. The present study focuses on analyzing the compositional aspects of ECM assembly and presents a new imaging method, TL-CRM, for analysis of the macromolecular interactions of collagen and other natural biopolymers as they assemble into complex 3D matrices.

Complex 3D collagen-based matrices, which are commonly used as cell culture substrates and are amenable to tissue engineering applications, must have specific compositional and structural properties that support tissue-specific cell attachment, proliferation, migration, and differentiation. Previously, we found that

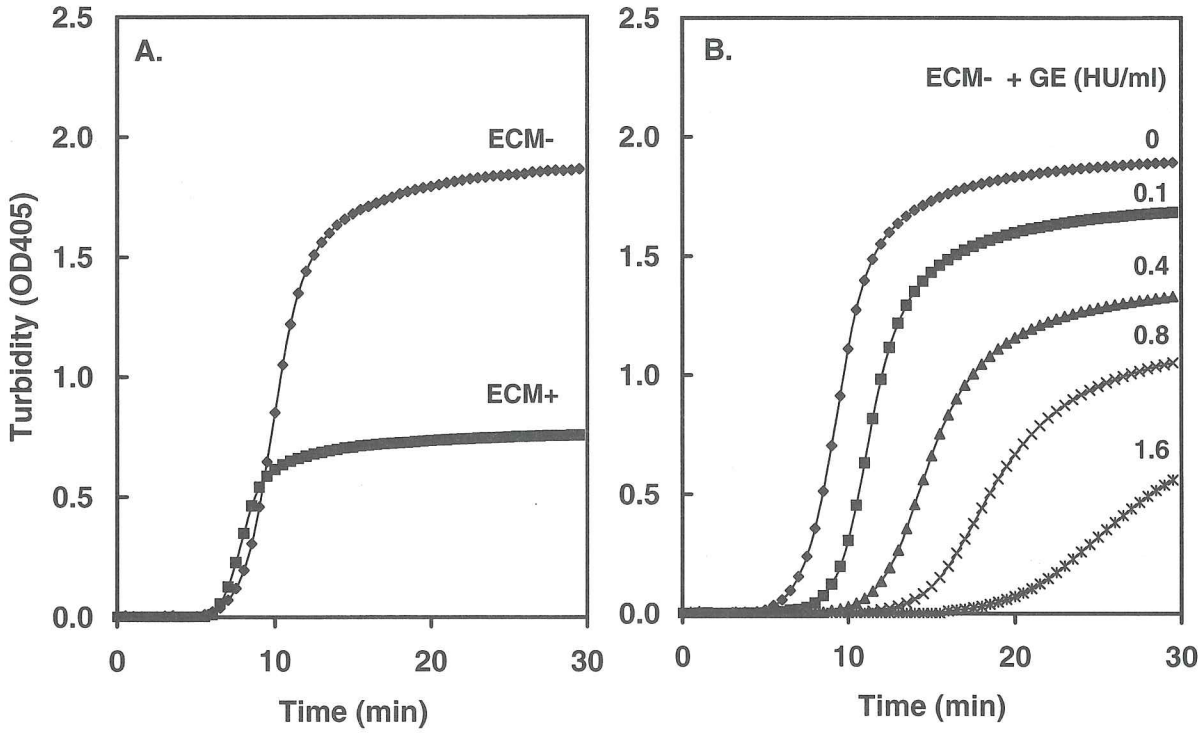

FIGURE 13 Spectrophotometric turbidity measurements of fibrillogenesis and matrix assembly of interstitial ECM in the presence and absence of PG/GAG components. Assembly of interstitial ECM prepared from intestinal submucosa before (ECM+) and after (ECM−) extraction of PG/GAG components (A). Assembly of ECM− at a collagen concentration of 1.0 mg/mL in the presence of extracted PG/GAG components at concentrations ranging from 0 to 1.6 HU/mL (B).

specific cell types responded differently when grown in vitro on matrices formed from interstitial ECM vs purified type I collagen.[9] Upon evaluation of these two matrices using routine SEM analysis, considerable disparity in the structure of individual fibrils as well as in their organization was identified. However, because these matrices possess a significant water content, structural artifacts introduced during specimen processing, such as shrinkage due to critical point drying, were a concern. Confocal reflection microscopy provides a method for studying the architecture of biopolymer matrices in a hydrated state without the requirement for extensive specimen manipulation. Unlike conventional microscopy techniques, CRM also provides microstructural information in 3D rather than 2D. We now report a first application of CRM in a time-lapse mode for the evaluation of the kinetic and structural properties of ECM-based biopolymers as they assemble from a soluble to a gel phase.

Results obtained with TL-CRM showed that type I collagen and interstitial ECM matrices differed with respect to their 3D fibril morphology and organization as well as their kinetic parameters of assembly (e.g., length of lag phase and rate of polymerization). More specifically, when compared at the same collagen concentration, interstitial ECM showed an increased rate of assembly, decreased time of nucleation (lag phase), increased density, and decreased diameter of fibrils. Compositional analysis of the reconstituted interstitial ECM matrix shows that it contained at least three different collagens. Collagen types I and III were predominant, with lesser quantities of type V (S. L. Voytik-Harbin, unpublished). Although the full portfolio of GAGs, PGs, and glycoproteins present in this reconstituted matrix have not been defined, several members of these macromolecular families have been identified in the starting material, intestinal submucosa. Five types of GAGs, including heparin sulfate, hyaluronic acid, chondroitin sulfate A, dermantan sulfate, and heparin, have been identified in intestinal submucosa.[14] Preliminary evidence also suggest that intestinal submucosa contains the PGs decorin and heparan sulfate proteoglycan as well as the glycoprotein fibronectin.[24] The presence of multiple types of collagen, PGs, and GAGs in the reconstituted interstitial ECM and the studies indicating their effects on collagen assembly suggested that these components might be responsible for the differences in matrix architecture and assembly from that of type I collagen alone.

PGs and GAGs are important structural and signaling components of connective tissue ECM and are known to influence fibrillogenesis and matrix architecture.[25] Early studies of developing tendon used histochemical stains in EM to correlate fibril diameters and periodicities in the tissue with PG and GAG content.[26] Of GAG molecules, heparin is the best characterized regarding its interactions with collagen and its effects on matrix assembly.[27–32] This is likely due to the dramatic effects observed when heparin is combined with type I collagen and to the fact that, with the exception of hyaluronic acid, the other GAG molecules are usually present as component elements of proteoglycan molecules. TL-CRM demonstrated a dose-dependent increase in the rate of collagen fibrillogenesis with heparin addition. Collagen fibrils formed in the presence of heparin were increased in diameter and decreased in density. These findings are consistent with previous studies using transmission and scanning EM, whereby heparin was found to induce a dose-dependent increase in fibril size of self-assembled type I collagen matrices, giving rise to a more porous but less cohesive matrix.[31] This effect appeared to be unique to heparin in comparison with several other GAG components of the ECM.[30]

Interactions between the PG decorin and type I collagen have been shown also to influence the kinetics of collagen fibrillogenesis as well as the diameter of and the distance between fibrils both in vitro[19–21,33–35] and in vivo.[22,26] In the present study, the addition of decorin to type I collagen at a ratio of 1:20 was found to increase the lag phase or nucleation time by TL-CRM and the routinely used turbidity assay. These results are consistent with previous studies in which the effect of decorin on the kinetics of type I collagen fibrillogenesis was studied by turbidity assay alone.[19,20] Unfortunately, the turbidity assay provides no information on the nature or orientation of the collagen fibril. Separate studies involving negative staining and SEM suggested that decorin from bovine tendon yielded collagen fibrils that were structurally decreased in diameter.[35] More recently, Kuc and Scott found decorin to increase diameters of fibrils formed.[33] With TL-CRM, no difference in matrix architecture due to the addition of decorin to type I collagen at ratios of 1:20 and 1:80 was observed. The discrepancy in these results might be attributed to artifacts due to specimen processing for structural observations, variation in GAG chain (e.g., degree of glycosylation),[34] tissue origin of decorin,[19,33] and differences in assembly conditions (e.g., buffer).[36,37]

For these studies, the application of both TL-CRM and the routine spectrophotometric-based turbidity assay allowed determination of consistency and correlation between results as well as the identification of new information provided by TL-CRM. In studies where concentration, but not composition, of molecules was evaluated, increases in optical density mea-

surements of turbidity or average pixel values of TL-CRM images consistently and accurately correlated with increased fibril density as measured by TL-CRM. However, neither optical density measurements nor average pixel values were reliable in predicting or comparing fibril density of matrices differing in composition. This discrepancy is likely due to the fact that light scattering (reflection) properties of collagen fibrils can be altered biochemically and/or biophysically with the composition and structure of the fibril. This observation is strong evidence warranting complete analysis, kinetic as well as 3D structural, of matrices for fuller understanding of their unique architectural properties. At this time, only TL-CRM has the capability for such complete analysis without deleterious specimen manipulation.

The simultaneous collection of structural and kinetic information offered by TL-CRM allows quantitation of specific fibril properties (e.g., fibril diameter) and provides additional insight into the mechanisms of self-assembly including the determination of number of nucleation sites and the occurrence of fibril bundling. As with fluorescence-based imaging, TL-CRM is a very sensitive technique—it benefits from the fact that although some very small reflecting particles or fibrils cannot be resolved (according to the Rayleigh criterion), they still can be detected and visualized. Based upon the Rayleigh criterion, the calculated resolution for our CRM system was 212 nm. Interestingly, the x–y resolution of a microscope operating in reflected light mode is not improved by the confocal iris, but the contrast transfer characteristics for fine detail is much better than in the case of a nonconfocal microscope.[38] In these studies, optimized fibril contrast scanning distances ranged from 20 to 50 μm from the coverslip. Depth intensity of the fibril contrast was diminished at deeper focus levels, indicating substantial scattering and refraction of the laser intensity. Although offering resolution that is significantly less than that of SEM (2–8 nm), CRM readily provided 3D spatial information and did not require extensive processing techniques (e.g., physical sectioning and staining). High-throughput computer algorithms for quantitation of various fibril and matrix parameters, including diameter, length, degree of curvature, and orientation within the matrix, are currently under development.

The authors wish to thank Monica Shively and Steve Kelley for their excellent technical assistance with the confocal microscope and image analysis.

REFERENCES

1. Comper, W. D.; Veis, A. Biopolymers 1977, 16, 2133–2142.
2. Comper, W. D.; Veis, A. Biopolymers 1977, 16, 2113–2131.
3. Kadler, K. E.; Holmes, D. F.; Trotter, J. A.; Chapman, J. A. Biochem J 1996, 316, 1–11.
4. Holmes, D. F.; Watson, R. B.; Kadler, K. E. Biochem Soc Trans 1991, 19, 808–811.
5. Miyahara, M.; Hayashi, K.; Berger, J.; Tanzawa, K.; Njieha, F. K.; Trelstad, R. L.; Prockop, D. J. J Biol Chem 1984, 259, 9891–9898.
6. Miyahara, M.; Njieha, F. K.; Prockop, D. J. J Biol Chem 1982, 257, 8442–8448.
7. McBride, D. J., Jr.; Kadler, K. E.; Hojima, Y.; Prockop, D. J. Matrix 1992, 12, 256–263.
8. Friedl, P.; Maaser, K.; Klein, C. E.; Niggemann, B.; Krohne, G.; Zanker, K. S. Cancer Res 1997, 57, 2061–2070.
9. Voytik-Harbin, S. L.; Brightman, A. O.; Waisner, B. Z.; Robinson, J. P.; Lamar, C. H. Tiss Eng 1998, 4, 157–174.
10. Allen, T. D.; Schor, S. L.; Schor, A. M. Scan Electron Microsc 1984, Pt 1, 375–390.
11. Keith, C. H.; Bird, G. J.; Farmer, M. A. Biotechniques 1998, 25, 858–866.
12. Semler, E. J.; Tjia, J. S.; Moghe, P. V. Biotechnol Prog 1997, 13, 630–634.
13. Gunzer, M.; Kampgen, E.; Brocker, E. B.; Zanker, K. S.; Friedl, P. Adv Exp Med Biol 1997, 417, 97–103.
14. Hodde, J. P.; Badylak, S. F.; Brightman, A. O.; Voytik-Harbin, S. L. Tiss Eng 1996, 2, 209–217.
15. Voytik-Harbin, S. L.; Brightman, A. O.; Kraine, M. R.; Waisner, B.; Badylak, S. F. J Cell Biochem 1997, 67, 478–491.
16. Wiechelman, K. J.; Braun, R. D.; Fitzpatrick, J. D. Anal Biochem 1988, 175, 231–237.
17. Marotta, M.; Martino, G. Anal Biochem 1985, 150, 86–90.
18. Bjornsson, S. Anal Biochem 1993, 210, 282–291.
19. Vogel, K. G.; Paulsson, M.; Heinegard, D. Biochem J 1984, 223, 587–597.
20. Schonherr, E.; Hausser, H.; Beavan, L.; Kresse, H. J Biol Chem 1995, 270, 8877–8883.
21. Weber, I. T.; Harrison, R. W.; Iozzo, R. V. J Biol Chem 1996, 271, 31767–31770.
22. Danielson, K. G.; Baribault, H.; Holmes, D. F.; Graham, H.; Kadler, K. E.; Iozzo, R. V. J Cell Biol 1997, 136, 729–743.
23. Birk, D. E.; Linsenmayer, T. F. In Extracellular Matrix Assembly and Structure, Yurchenco, P. D., Birk, D. E., Mecham, R. P., Eds., Academic Press: San Diego, 1994; pp. 91–128.
24. McPherson, T. B.; Badylak, S. F. Tiss Eng 1998, 4, 75–83.
25. Iozzo, R. V. Annu Rev Biochem 1998, 67, 609–652.

26. Scott, J. E.; Orford, C. R.; Hughes, E. W. Biochem J 1981, 195, 573–581.
27. Wood, G. C. Biochem J 1960, 75, 605–612.
28. Mathews, M. B.; Decker, L. Biochem J 1968, 109, 517–526.
29. Obrink, B. Eur J Biochem 1973, 33, 387–400.
30. McPherson, J. M.; Sawamura, S. J.; Condell, R. A.; Rhee, W.; Wallace, D. G. Coll Relat Res 1988, 8, 65–82.
31. Guidry, C.; Grinnell, F. J Cell Biol 1987, 104, 1097–1103.
32. Keech, M. K. J Biophys Biochem Cytol 1961, 9, 193–209.
33. Kuc, I. M.; Scott, P. G. Connect Tissue Res 1997, 36, 287–296.
34. Sini, P.; Denti, A.; Tira, M. E.; Balduini, C. Glycoconjugate J 1997, 14, 871–874.
35. Vogel, K. G.; Trotter, J. A. Coll Relat Res 1987, 7, 105–114.
36. Pogany, G.; Hernandez, D. J.; Vogel, K. G. Arch Biochem Biophys 1994, 313, 102–111.
37. Williams, B. R.; Gelman, R. A.; Poppke, D. C.; Piez, K. A. J Biol Chem 1978, 253, 6578–6585.
38. Oldenbourg, R.; Terada, H.; Tiberio, R.; Inoue, S. J Microsc 1993, 172, 31–39.